A Vector-Based Approach for Dimensioning Small Cell Networks in Millimeter-Wave Frequencies

Jianming Zhang, Deru Zhang, and Juanjuan Sun

***Abstract*—Millimeter wave (mmW) is being deployed in hotspot scenarios for providing high bandwidths. However, the coverage of mmW cell is limited due to the rapid attenuation during the propagation and sensitivity to blockage by obstacles. In this paper, we propose a novel dynamic programming approach for automated dimensioning and appropriate placement of mmW small cells (SCs) in dense urban under the constraints of coverage and budget. Being cognizant of the blockage by city buildings, a fast search algorithm based on vector is introduced to enable most line-of-sight (LOS) communication links between base stations (BSs) and mobile stations (MSs). The analysis of time complexity is also derived in closed forms. The evaluation of our approach was carried out in both hypothetic and realistic scenarios. Results show that the studied model is effective for a real large-scaled network and 4 or 5 times faster than the conventional ones based on grid-map.**

***Index Terms*—Dimensioning, millimeter wave, radio network planning, small cell.**

I. Introduction

With the emergence of new radio access technologies, like massive multiple-input multiple-output (MIMO), ultra-dense network (UDN), mmW communication, and so on [1], the capacity of wireless network has been far scaled to supply the ever-growing service demands of MSs. When it comes to the application of new technologies, one major concern for the network operator is how to control the capital expenditure (CAPEX) and operational expenditure (OPEX) costs.

It is reported that the total number of global mobile users will grow up to 5.7 billion, and the average mobile connection speed will be 43.9 Mbps by 2023 [2]. Radio network planning (RNP) is an essential operation when the operators are continuously upgrading their networks, and it significantly determines the acquired system performance and the required costs [3]–[5]. One example is presented in [6] where the coverage and service quality of the Klaten city were improved by adding as few additional BSs as possible using a cell planning software. The acquired coverage, traffic throughput and delay vary with deploying schemas just like the works reported by [7], [8].

Manuscript received 8 June 2021; revised 24 December 2021 and 28 February 2022; accepted 26 April 2022. Date of publication 23 May 2022; date of current version 15 August 2022. This work was supported by the National Key Research and Development Program of China under Grant 2020YFF0305601. The review of this article was coordinated by Dr. Xiaohu Ge. *(Corresponding author: Jianming Zhang.)*

The authors are with the School of Electronic Engineering, Beijing University of Posts and Telecommunications, Beijing 100876, China (e-mail: jmzhang@bupt.edu.cn; drzhang@bupt.edu.cn; sunjj@bupt.edu.cn).

Digital Object Identifier 10.1109/TVT.2022.3176622

Exploring new spectrum bands of mmW [9], [10] is a promising solution to scale network capacity. However, since the wavelength shrinks by an order of magnitude compared with the microwave, mmW suffers from greater attenuation [9], [11], [12]. Measurements showed the penetration loss of common building materials from 20 to 50dB [13], the diffraction loss over rooftop from 10 to 80dB [14], the rain attenuation with a few dB/km [15].

Further, ultra-dense cells are deployed in partial hotspot areas to meet wireless traffic volume. In fact, the ultra-dense network is being proposed to be deployed in overall scenarios based on the mmW technologies nowadays [16]. Not only the capacity and coverage but also CAPEX costs increase with the growth of cell densities [17], [18]. The lower power is transmitted, and the longer battery life is achieved in the dense network scenario [19]. It is shown in [20] that femtocells present a lower carbon footprint than the macro cells in terms of yearly tons of CO^2 per km^2 in high density and capacity networks but higher CAPEX.

A. Related Work

The application of mmW and UDN makes the cell size smaller than before. The mmW cell is expected to provide limited coverage on the order of 200 m which means high terrain costs must be incurred by the network operators [21]. Many studies have considered network planning to meet the coverage and traffic demand while reducing the overall costs. The objective is to select a subset of candidate sites to meet the network performance metrics that is essentially a set covering problem with NP-Hard complexity [22]. Thus, heuristic solutions, like simulated annealing approach [23], genetic algorithm [24], particle swarm optimization (PSO) algorithm [25], [26], etc., are proposed for cell selection and configuration in most of the works.

Considering the significant amount of computation time as the number of candidate sites increases, more simplified approaches have also been presented in the literature. Clustering strategies based on k-means to deploy a heterogeneous network have been proposed in [27]. Taking into account the stochastic body blockage, in [28], a greedy algorithm has been presented to find the approximation solution of cell location and antenna direction. The author showed that the approximation and optimal solutions are close in dimension. A linear equation system was set up to config the cell locations and frequencies under the signal-to-interference plus noise ratio (SINR) constraint in [29]. The author used Z-order curve which converts three-dimensional

points in geographic areas into unidimensional ones. The time-consuming is still large because the coverage and intersecting areas of cells were estimated grid by grid. Nonlinear programming problems to find the optimal set of BSs have been investigated in [30], [31]. In [30], the nonlinear objective function as well as nonlinear inequality constraints based on SINR uncertainty due to fading has been involved. An iterative method to optimize the site placements was introduced which moves the locations of BSs in the steepest descent direction of the objective function. In [31], a constrained convex optimization system to minimize the cardinality of sites which satisfying the sum rate requirement has been presented. The author converted the optimization problem into a sequence of minimization problems solved by the logarithmic barrier method. In [32], two-level network planning has been proposed to simplify the problem which optimizes the number of BSs in the first level and deploys locations and powers in the second level. In [33], [34], self-dimensioning and BS on/off switching by traffic zooming have been introduced which can be solved by greedy algorithm for large-scale networks.

Since it is necessary to evaluate the coverage rate of the given area, most strategies will split the area into a series of small areas and calculate the signal level or SINR in each small area. Evenly dividing into small grids is a frequently-used approach. But the higher the division accuracy, the greater the number of grids that need to be evaluated. In [35], based on the Manhattan-type geometry (MTG) scenario, the author designed a low-complexity mmWave BS deployment algorithm by establishing a closed-form expression of network connectivity and building size, transmit power, building density, and BS density. Although a special disk-shaped blockage free regions (BFR) model is created, it is still time-consuming to evaluate the signal level of all grids in sequence. Based on a smart simulated annealing approach, the author of [36] designed two SC displacement schemes, random displacement approach and probed displacement approach, to find the optimal SC sites. However, it also needs to calculate the coverage rate grid by grid, and worse still, once the fitness function is calculated, the coverage quality of all grids must be calculated again. In addition, for the deployment of small cells in a heterogeneous network, the author proposed a joint optimization algorithm for spectrum efficiency metric (SM), energy efficiency metric (EM), and deployment cost efficiency metric (DM) in [37]. But the calculation of the proposed joint objective function is also grid-by-grid and time-consuming.

B. Motivations and Contributions

In most research, the planning area is uniformly split into grids because the computer is better at working with discrete data than continuous data. Most works estimate signal level or SINR grid by grid that may produce an enormous computation cost and are inefficient for a large-scale network. Moreover, empirical propagation models are used for calculating path loss which may cause relatively large errors in the scenario of mmW system. The impact of terrain blockage in the mmW links shouldn't be ignored in urban city. [28] provided a method to model the stochastic blockage in the radio link and a greedy algorithm to solve stochastic optimization equations. However, the work didn't consider the blockage of geographic topology but only human body.

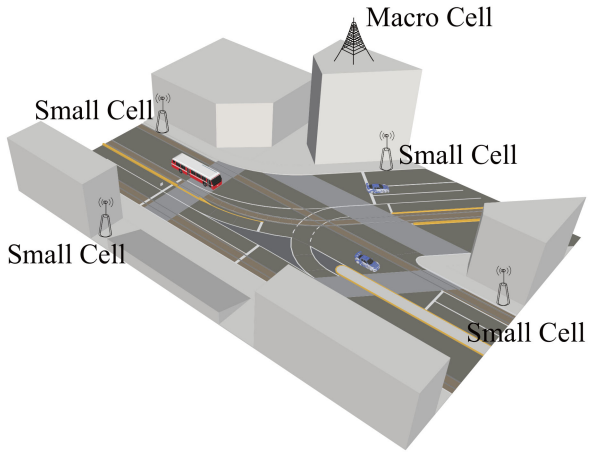

Fig. 1. Small cells in dense urban.

The scope of this work is to find the minimum number of mmW cells and optimally locate them in the real urban street scenario. The presented solution formulates SCs placement problem subject to network coverage constraints. We explicitly account for the geographic topologic nature and computation complexity. The main contributions of this work are summarized below:

1) We propose a method of evaluating cell coverage based on vector that is expected to reduce calculation amount.
2) We consider geographic topology and calculate the signal level with exact radio ray tracing rather than with empirical statistical models.
3) We introduce a dynamic programming approach to solve the cell placement problem and mathematically derived the computation complexity.
4) We present the simulation results of our proposed solution in both hypothetic and realistic scenarios with 28 G, 39 G, 60 GHz frequencies.

The rest of the paper is organized as follows. Section II presents the system model and necessary propagation formulas. Afterwards, Section III introduces our solution to mmW cell placement problem, and Section IV provides the simulation results and analysis. We finally conclude this paper in Section V.

II. Problem Description and System Model

A. Problem Definition

As we know, there are dense buildings such as malls, residential towers, office buildings, and others in the central urban. SCs are proposed to be densely placed in to improve the capacity and signal quality of MS as shown in Fig. 1. Moreover, mmW is expected to be deployed as it offers a large number of frequency spectra that can offer high network capacity. The objective is to find the minimum set of cell locations subject to the network coverage constraints in the urban street scenarios.

The mmW loses its intensity rapidly as it enters an enclosed building by wall penetration because the E-filed transmission

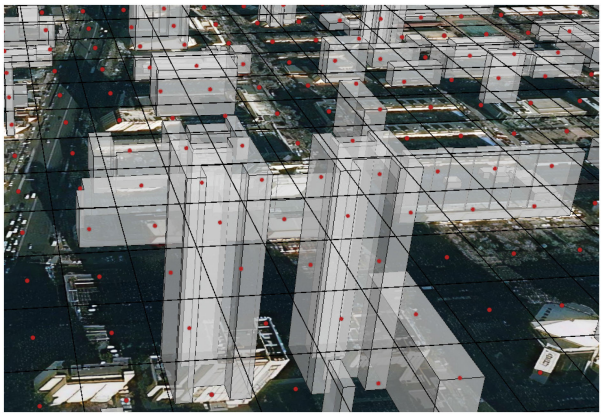

Fig. 2. Geographic rasterization.

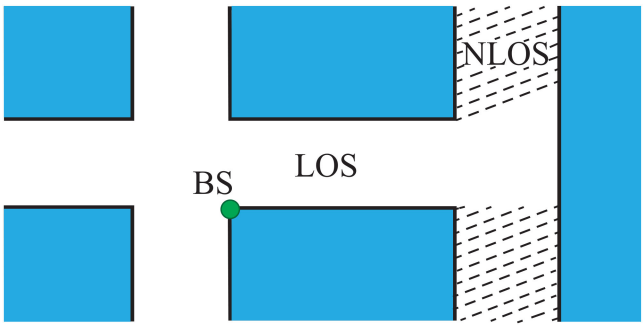

Fig. 3. City street canyon.

coefficient falls with frequency [38]. For the sake of energy-saving and carbon emission, it is improper to cover the indoor by absolutely increasing the transmission power of outdoor BSs. Therefore, we focus on maximizing the outdoor coverage but not outdoor-to-indoor coverage. The indoor distribution systems or base stations are commonly used for hardly covered indoor areas, but that is beyond the scope of this work.

In most works, the planning area is split into grids with the specified resolution such as 1 m or 5 m as illustrated in Fig. 2. It is an NP-Hard problem to choose the minimum BSs covering all grids. In this paper, we proposed coverage metrics based on vector instead of grid and applied a dynamic programming approach to solve the cell placement problem. Computation complexity is derived in closed form.

B. System Model

The coverage area of urban streets is characterized by linear distribution along streets and building blocks. Radio wave that always travels in a straight line attenuates severely while falling across barriers. As shown in Fig. 3, the open spaces outside get good signal footprints while the shaded area is weakly covered by the BS. We consider the outer contours of buildings as the coverage boundary since the street area out of the buildings will be expected to be in good coverage if the received signal at the building's boundaries is strong enough.

As mentioned above, cells boundaries, but not signal footprints of all grids, are estimated in this paper. In the scenario of streets, the coverage border of a millimeter wave SC can be evaluated by the signal levels of walls. The outer contour of a building is modeled as a polygon. There are a variety of properties of a building such as material, color, and more. The outer walls and their geometric features are the concerns of the proposed algorithm. Thus, given a geographic area, the outer walls of buildings are expressed as a set, $\mathbf{W} = \{w_1,\ w_2,\ \cdots, w_{|\mathbf{W}|}\}$, where w_i is defined as a line segment which is one edge of a building polygon. For a specific wall, which side faces the street should be clearly given. $w.\vec{\eta}$ is used to represent the outward normal of a wall.

Given a candidate set $\mathbf{X}$ of all possible SCs, $\mathbf{\Gamma}$ is the set of selected cells to cover the planning area. The aim is to find a minimum subset $\mathbf{\Gamma}$ from $\mathbf{X}$ under the coverage constraint. Each candidate cell has two states: used or not. This is considered as an NP-Hard problem that requires a running time of $O\left(2^{|\mathbf{X}|}\right)$.

C. Propagation Model

For a radio link, the received signal power is given in Equation (1):

$$P_{\mathrm{RX}} = P_{\mathrm{TX}} + G_{\mathrm{TX}} + G_{\mathrm{RX}} - L_{\mathrm{PL}} - L_{\mathrm{Rain}} - z \cdot \sigma_{\mathrm{SF}}, \quad (1)$$

where P_{RX} represents the received power in dBm, G_{TX} and G_{RX} are the gains of transmitting antenna and receiving antenna respectively, L_{PL} is the path loss of signal propagation, L_{Rain} is the rain attenuation, z is a zero-mean unit-variance Gaussian random variable, and σ_{SF} is the standard deviation of shadow fading. In the scenario of urban streets, the path loss L_{PL} of LOS was provided in 3GPP TR 38.901 [39] as

$$L_{\mathrm{LOS}} = 32.4 + 21\log_{10}(d) + 20\log_{10}(f_c), \quad (2)$$

where d is the path length and f_c is the frequency. In the non-line-of-sight (NLOS) case, we compute the path loss caused by diffractions or reflections. The additional diffraction loss can be computed by the GTD model [40] as

$$L_{\mathrm{D}} = 20\log_{10}\left(\frac{\sqrt{d_1 d_2 (d_1 + d_2)}}{d \cdot |D|}\right), \quad (3)$$

where the diffraction loss is denoted by L_D, D is the diffraction coefficient independent of distance, d_1 and d_2 respectively denote the propagation path lengths before and after diffraction, d is the direct 3-dimensional distance between the transmitting source and the diffracted wave. The GTD model can be divided into a distance-dependent part and a distance-independent part which is rewritten by

$$L_{\mathrm{D}} = 20\log_{10}\left(\frac{\sqrt{d_1 d_2 (d_1 + d_2)}}{d}\right) + L_{\mathrm{DC}}, \quad (4)$$

where $L_{\mathrm{DC}} = -20\log_{10}(|D|)$. The work in [14] presented the diffraction propagation measurements of mmWave and proposed a linear approximation of L_{DC} which is relative to the frequency and diffraction angle. The additional path loss caused by reflections is denoted by E-field reflection coefficient $L_R = -20\log_{10}(|R|)$. The values of R for transverse electric (TE) and

transverse magnetic (TM) polarization are respectively calculated by Equations (5) and (6) in [38]:

$$R_{TE} = \frac{\cos\theta - \sqrt{\eta - \sin^2(\theta)}}{\cos\theta + \sqrt{\eta - \sin^2(\theta)}}, \tag{5}$$

$$R_{TM} = \frac{\eta\cos\theta - \sqrt{\eta - \sin^2(\theta)}}{\eta\cos\theta + \sqrt{\eta - \sin^2(\theta)}}. \tag{6}$$

Due to the high density of SCs, the users will be disturbed by other adjacent SCs in the downlink transmission. So, it is also necessary to evaluate the downlink SINR in the planning area. For UE_k, which is served by SC_i, $SINR_k$ is given by the following formula [41]:

$$\begin{aligned} SINR_k &= \frac{P_{TX_i} G(\theta,\delta) h_i L_{PL_i}}{I + \sigma^2} \\ &= \frac{P_{TX_i} G(\theta,\delta) h_i L_{PL_i}}{\sum_{j=1, j\neq i}^{N_{SC}} P_{TX_j} \zeta_{j,t} h_j L_{PL_j} + \sigma^2}, \end{aligned} \tag{7}$$

where P_{TX_i} is the transmit power of SC_i, $G(\theta,\delta)$ represents the combined gain of SC_i to UE_k which uses directional beamforming, $h_i \sim exp(1)$ denotes the small scale Rayleigh fading from SC_i to UE_k, $\zeta_{j,t}$ is an indicator showing whether SC_j is transmitting at time slot t (i.e., $\zeta_{j,t} = 1$) or not (i.e., $\zeta_{j,t} = 0$), N_{SC} is the total number of SCs in the planning area and σ^2 denotes noise power.

D. SCs Placement Problem

Let $P_{\mathrm{RX}}(i,j)$ denote the received power at the wall w_j from the cell i which is calculated by Equation (1). $c_{i,j} = 1$ if $P_{\mathrm{RX}}(i,j) > P_{\min}$ where $P_{\min}$ is the minimum required signal power, otherwise $c_{i,j} = 0$. The set $\mathbf{S}_i$ of all covered walls by the cell i is defined as

$$\mathbf{S}_i = \{w_j : \forall c_{ij} = 1, \forall 1 \le j \le |\mathbf{W}|\}. \tag{8}$$

All the coverage sets form a set family $\boldsymbol{\mathcal{F}} = \{\mathbf{S}_1, \mathbf{S}_2, \cdots \mathbf{S}_{|\mathbf{X}|}\}$. $\boldsymbol{\Gamma}(\boldsymbol{\Gamma} \subset \mathbb{N})$ is the set of the selected SCs' numbers that are subject to the coverage constraints. The coverage sets of all SCs in the feasible solution $\boldsymbol{\Gamma}$ form a family of sets $\boldsymbol{\mathcal{L}}(\boldsymbol{\mathcal{L}} \subseteq \boldsymbol{\mathcal{F}})$. The aim is to find the minimum $|\boldsymbol{\Gamma}|$ and $|\boldsymbol{\mathcal{L}}|$. Note that it's supposed that one wall can be entirely covered by one cell. If it couldn't be, the wall should be split into segments.

III. Dynamic Programming for the Small Cell Locations

There are two high time-consuming procedures in this problem: setting up a large-scale matrix $\{c_{ij}\}_{|\mathbf{X}|\times|\mathbf{W}|}$ and finding the optimal set $\boldsymbol{\Gamma}$. An exhaustive search for $\boldsymbol{\Gamma}$ and $\{c_{ij}\}$ needs at least $O\left(2^{|\mathbf{X}|\times|\mathbf{W}|}\right)$ time. In fact, we don't have to calculate every value of $\{c_{ij}\}$ because an SC can't cover the walls far away or deeply blocked. There is no need to do an exhaustive search for $\boldsymbol{\Gamma}$ as well because only a few cells can be the candidate serving cells of a designated wall.

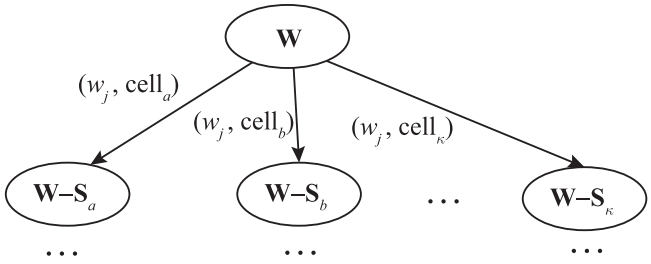

Fig. 4. A recursive tree of the wall set $\mathbf{W}$.

A. A Recursive Procedure

There is an optimal substructure to this problem.

Theorem 1: If an optimal solution $\boldsymbol{\Gamma}^*$ has a subset $\boldsymbol{\Gamma}'$ covering the walls $\bigcup_{i\in\boldsymbol{\Gamma}'} \mathbf{S}_i$, then $\boldsymbol{\Gamma}'$ must be an optimal solution to the subproblem of covering $\bigcup_{i\in\boldsymbol{\Gamma}'} \mathbf{S}_i$.

Proof of Theorem 1. The proof is given in Appendix A.

Given a wall subset $\mathbf{W}$, we try to find the serving cell for each wall and then get a solution for $\mathbf{W}$. The cells which cover a wall, say w_j, form a set $\boldsymbol{\Gamma}(w_j)$ defined as

$$\boldsymbol{\Gamma}(w_j) = \{i : \forall c_{i,j} = 1\}. \tag{9}$$

Suppose for a designated wall w_j, one cell of $\boldsymbol{\Gamma}(w_j)$, say i, is the cell of an optimal solution. Then the left uncovered walls are $\mathbf{W} - \mathbf{S}_i$. As long as we test all candidate cells in $\boldsymbol{\Gamma}(w_j)$ and find the optimal solutions covering the set $\mathbf{W} - \mathbf{S}_i$, an optimal solution for $\mathbf{W}$ is guaranteed to be obtained.

Pick the subproblem domain as searching an optimal set of cells covering the walls $\mathbf{W}'$ where $\mathbf{W}' \subseteq \mathbf{W}$. We define $e(\mathbf{W}')$ as the expected number of serving cells covering $\mathbf{W}'$. Obviously, $e(\mathbf{W}') = 0$ when $\mathbf{W}' = \varnothing$. Take any one wall w_j of $\mathbf{W}'$ and cell i where $i \in \boldsymbol{\Gamma}(w_j)$ when $\mathbf{W}' \neq \varnothing$. Given the coverage set $\mathbf{S}_i$ of cell i, we get $e(\mathbf{W}') = e(\mathbf{W}' - \mathbf{S}_i) + 1$. The above process assumes that we know which cell i of $\boldsymbol{\Gamma}(w_j)$ is in an optimal solution. A recursive formulation is given as follows:

$$e(\mathbf{W}') = \begin{cases} 0 & \mathbf{W}' = \varnothing \\ \min\limits_{i\in\boldsymbol{\Gamma}(w_j)} \{e(\mathbf{W}' - \mathbf{S}_i) + 1\} & w_j \in \mathbf{W}', \mathbf{W}' \neq \varnothing \cdot \end{cases} \tag{10}$$

The order in which we chose the wall w_j and the cell i is essential. The recursive procedure is expressed as a search tree as shown in Fig. 4. There is a set of uncovered walls that is denoted by the status of tree nodes. We expand a tree node by choosing an uncovered wall and its serving cells in optimal solutions. With the cells being added into the solution, the status changes until all walls are covered. However, it is unknown whether an SC is in an optimal solution during the process. Hence, we adopt minimum benefit maximization strategy here to traverse the tree.

According to the upper bound of approximation ratio (see in Section III-C), it's sensitive to the effective coverage rate of selected cells. Suppose BSs uniformly distributed over the whole planning area, the walls located at the edge of the area can be covered by the least cells and these cells likely have the minimum coverage area. Searching process starts from the wall which has the least serving cells.

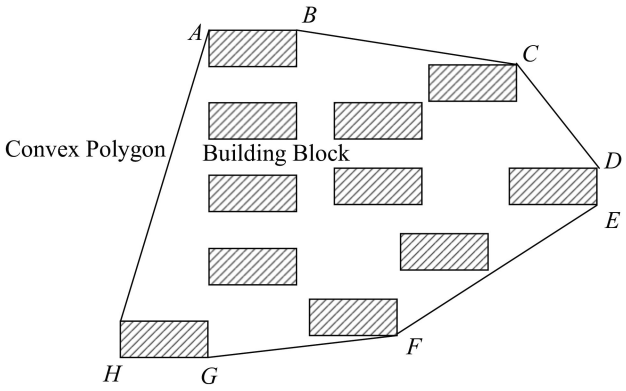

Fig. 5. Convex polygon.

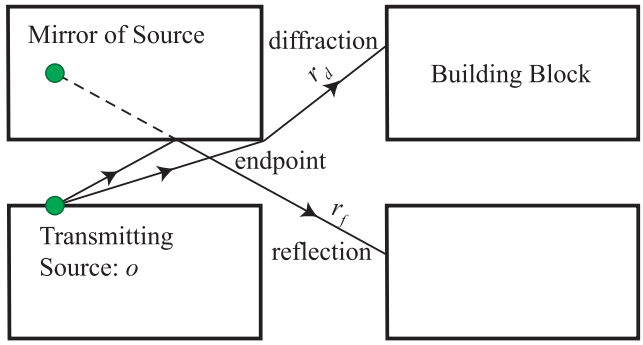

Fig. 6. Diffraction and reflection.

First, we construct a tight convex polygon P to enclose all walls in $\mathbf{W}$ as shown in Fig. 5. The work in [42] has proved that the convex polygon of a set of n points can be computed in $O(n \log n)$ time. Then we select a wall w_j located at the corners of P and search for its serving cells $\mathbf{\Gamma}(w_j)$ to expand the tree. According to the minimum benefit maximization strategy, we just keep a small number of, say κ, branches which provide the most covered walls in LOS links for a large-scaled search tree.

The proposed steps are as follows:

1) generate the root of the search tree with the set $\mathbf{W}$ of uncovered walls;
2) choose the top node of untraversed nodes and an uncovered wall w_j which located at the edge of the planning area;
3) search for the set $\mathbf{\Gamma}(w_j)$ of candidate serving cells;
4) select κ cells from $\mathbf{\Gamma}(w_j)$ with the most walls in LOS links to expand the current tree node.
5) update the set of uncovered walls. If the coverage conditions are met, then exit; else, go on to step 2).

B. Determine the Candidate Cells

Millimeter wave suffers much higher propagation loss than microwave especially in NLOS scenarios. Considering the time consuming, we just evaluate the coverage areas where the wave can transmit in a straight line or a small number of diffractions and reflections from the cell location. On account of geometrical symmetry, the candidate serving cells of the wall w_j can be found in the propagation paths started from the wall. Here, we suppose the transmitting antennas of SCs are mounted on the walls. The process can be divided into the following steps:

1) Search for the walls in LOS: compute the maximum allowed propagation distance r by link budget, and then find the set $\mathbf{W}_{\text{LOS}}$ of walls in the LOS areas taken the concerned wall w_j as a center and r as the maximum search radius.
2) Search for the walls in diffraction: compute the maximum allowed secondary propagation distance r_d for the endpoints of every wall in $\mathbf{W}_{\text{LOS}}$ by link budget, and then find the set $\mathbf{W}_{\text{D}}$ of walls in LOS, taken the endpoints of the walls in $\mathbf{W}_{\text{LOS}}$ as virtual transmitting sources and r_d as the search radius as shown in Fig. 6.
3) Search for the walls in reflection: compute the maximum allowed secondary propagation distance r_f for every wall in $\mathbf{W}_{\text{LOS}}$ by link budget, and then find the set $\mathbf{W}_{\text{R}}$ of walls in LOS, taken the mirror points as virtual transmitting sources and r_f as the search radius as shown in Fig. 6.
4) Determine the candidate serving cells: search the cells which antennas are mounted on the walls in $\mathbf{W}_{\text{LOS}}$, $\mathbf{W}_{\text{D}}$ and $\mathbf{W}_{\text{R}}$, and select κ cells covering the most walls by directional LOS links.

In the above process, the search radius can be calculated by link budget using equations (1)–(6). The key and time-consuming step is to find all walls in the LOS areas of a source, say o. A simple method is: take each pair of walls, test whether one blocks another, and if so, exclude the wall segments blocked. This direct algorithm obviously requires $O(|\mathbf{W}|^2)$ running time. However, in most practical cases, the total number of blocked wall segments is much smaller than quadratic. Inspired by a commonly used sweeping algorithm, we proposed an algorithm which has a logarithmic time complexity to find the LOS walls.

Let the sector with a center o, radius $r_{\max}$ and angle range $[\theta_b, \theta_e)$ where $0 \leq \theta_b < \theta_e \leq 2\pi$ be the search area in which we want to find the walls in LOS. All the walls intersecting or inside the sector form a wall set $\mathbf{W}' = \{w_1, w_2, \ldots, w_{|\mathbf{W}'|}\}$. Given the two endpoints $v^{(0)}$ and $v^{(1)}$ of any one wall, say w_i, we convert their Cartesian coordinates to polar coordinates centered on o. Without loss of generality, we set that $v^{(1)}$ is in the counterclockwise direction of $v^{(0)}$, and say that $v^{(0)}$ is the right endpoint and $v^{(1)}$ is the left one. We use an imaginary ray starting from the origin o to sweep the whole sector by rotating counterclockwise from $\theta = \theta_b$ to $\theta = \theta_e$. While the sweeping ray rotates, we maintain the location sequence of walls intersected by the ray and compute the wall segments in LOS. An example of the procedure is shown in Fig. 7 .

Let the length of the sweeping ray be $r_{\max}$ computed by link budget, and there is a sequence of walls intersecting the sweeping ray that are denoted by the status. The nearest wall from o is in LOS, while the rests are in NLOS. With the sweeping ray rotating, the status changes at the endpoint of each wall, called as event point. The algorithm exports the nearest wall segment in LOS and updates the status only at the moment when the sweeping ray reaches an event point.

In a specific implementation, a data structure, called the event queue $\boldsymbol{\mathcal{E}}$, is used to store all event points. The event points in $\boldsymbol{\mathcal{E}}$ are sorted by angle in counterclockwise order. Another data structure, called $\boldsymbol{\mathcal{T}}$, is used to store the status of the sweeping

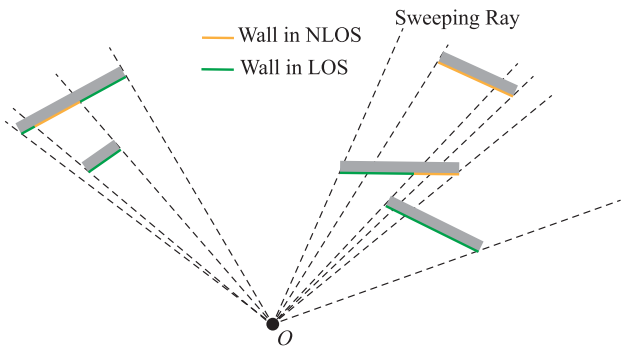

Fig. 7. Sweeping procedure.

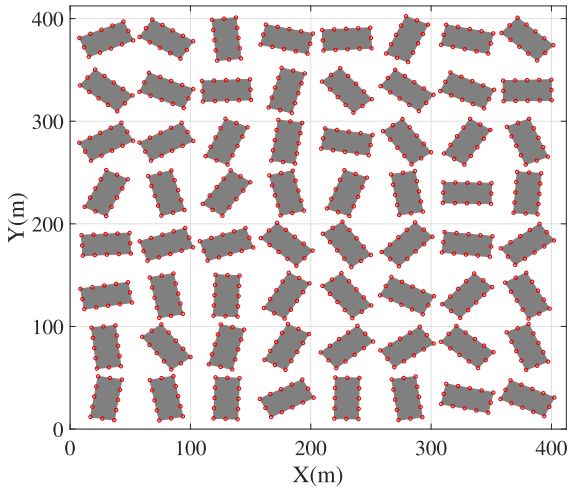

Fig. 8. Scenario 1: hypothetical dense urban area (The red circles represent the locations of candidate cells).

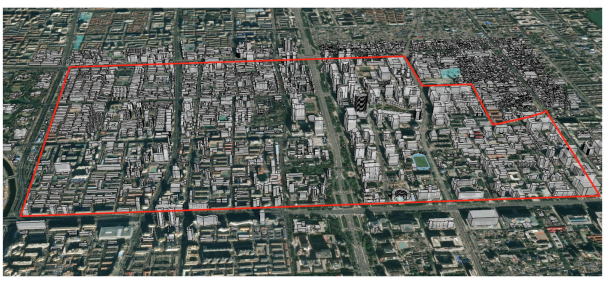

Fig. 9. Scenario 2: realistic dense urban area.

ray that is a distance-ordered sequence of walls intersecting the ray. $\mathcal{T}$ is dynamic and can be implemented by a balanced binary search tree.

The pseudocode of finding walls in LOS is presented in FindWalls.

UpdateStatus is the procedure of handling the event points and the operation for p in the algorithm is as follows:

1) If p is the right endpoint of a wall segment w, w will be inserted into $\mathcal{T}$ because the wall begins to intersect the sweeping ray. If w is in the front of $\mathcal{T}$, we'll report the last front wall or its fragment in LOS.

Algorithm: FindWalls.

Input: $\mathbf{W}$: The set of walls in the planning area; $\mathbf{SA}$: The swept area centered on o;
Output: The set of wall segments in LOS, $\mathbf{A}$

```
1  Function FindWalls(W, SA):
2      A ← ∅;
3      E ← ∅ ;    /* E is the event queue */
4      T ← ∅ ;    /* T is the status */
5      for each wall w ∈ W do
6          if w intersects or is inside SA then
7              insert its endpoints' polar coordinates into
               E;
8      while E ≠ ∅ do
9          select the next event point p in E, and erase it;
10         A = A ⋃ UpdateStatus(p,T) ;
11     return A;

12 Procedure UpdateStatus(p,T):
13     if p.w is a right endpoint then
14         insert p.w into T;
15         if p.w is in the front of T then
16             compute the point where the sweeping ray
               intersects the wall w' behind p.w, and
               report the last segment of w' in LOS;
17             set p as the start endpoint of one new
               segment in LOS;
18     else
19         if p.w is in the front of T then
20             report one segment of p.w where ends with
               p in LOS;
21             compute the point q where the sweeping
               ray intersects the wall w' behind p.w, and
               set q as the start endpoint of one new
               segment of w' in LOS;
22         remove p.w from T;
```

2) If p is the left endpoint of a wall segment w, we'll remove w from $\mathcal{T}$ because the wall doesn't intersect the sweeping ray any more. If w is at the head of $\mathcal{T}$, we'll report w or its fragment in LOS.

Lemma 1: Function FindWalls runs in $O(n \log n)$ time for n walls.

Proof of Lemma 1. The proof is given in Appendix B.

Based on FindWalls, the function of searching for the candidate serving cells of a designated wall w is presented in SearchCandidateCells.

Lemma 2: Given a point o, a set $\mathbf{W}$ of walls, and a set $\mathbf{X}$ of cells, the function SearchCandidateCells takes $O(|\mathbf{X}| \cdot |\mathbf{W}| + |\mathbf{W}|^2 \log |\mathbf{W}|)$ time at worst.

Proof of Lemma 2. The proof is given in Appendix C.

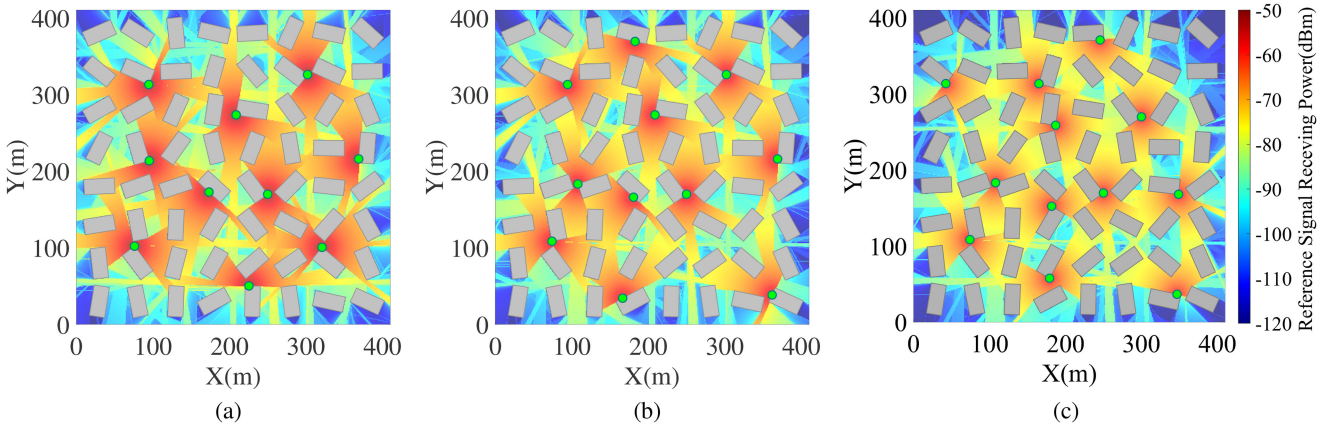

Fig. 10. Output cell locations and composite RSRP of 8 SCs assuming $\kappa = 4$. (a) 28 GHz. (b) 39 GHz. (c) 60 GHz.

Algorithm: SearchCandidateCells.

Input: o: The point to be covered; $\mathbf{W}$: The set of walls in the planning area; $\mathbf{X}$: The set of all possible cells;

Output: The set of cells which can cover o

Function `SearchCandidateCells` (o, $\mathbf{W}$, $\mathbf{X}$):
- initialize the wall sets $\mathbf{W}_{\text{LOS}} \leftarrow \varnothing, \mathbf{W}_{\text{D}} \leftarrow \varnothing, \mathbf{W}_{\text{R}} \leftarrow \varnothing$;
- compute the maximum allowed propagation distance by link budget, and construct a swept area $\mathbf{SA}0$;
- $\mathbf{W}_{\text{LOS}} =$ `FindWalls` ($\mathbf{W}$, $\mathbf{SA}0$);
- **for** *each wall* $w \in \mathbf{W}$ **do**
  - **for** *two endpoints of* w **do**
    - compute the allowed secondary propagation distance by diffraction link budget, and construct a swept area $\mathbf{SA}1$;
    - $\mathbf{W}_{\text{D}} = \mathbf{W}_{\text{D}} \bigcup$ `FindWalls` ($\mathbf{W}$, $\mathbf{SA}1$);
  - compute the mirror point o' of o;
  - compute the allowed secondary propagation distance by reflection link budget, and construct a swept area $\mathbf{SA}2$;
  - $\mathbf{W}_{\text{R}} = \mathbf{W}_{\text{R}} \bigcup$ `FindWalls` ($\mathbf{W}$, $\mathbf{SA}2$);
- **return** the cells located in $\mathbf{W}_{\text{LOS}} \bigcup \mathbf{W}_{\text{D}} \bigcup \mathbf{W}_{\text{R}}$;

Algorithm: AutoDeploySites.

Input: $\mathbf{W}$: The set of walls in the planning area; $\mathbf{X}$: The set of all possible cells; l_{un}: The allowed maximum sum of all uncovered wall's length; κ: The maximum expanded branches' number of a node in the search tree

Output: The set of selected cells which can cover the planning area

1. **if** *the total length of* W *is less then* l_{un} **then**
2. return $\varnothing$;
3. construct a convex polygon P enclosing all walls in $\mathbf{W}$;
4. select a vertex o at one corner of P;
5. C = `SearchCandidateCells` (o,$\mathbf{W}$,$\mathbf{X}$);
6. compute the coverage sets of all cells in $\mathbf{C}$;
7. remain at most κ cells covering the most walls in LOS;
8. $\mathbf{\Gamma}_{\text{min}} \leftarrow \varnothing$;
9. **for** *each cell* $c \in \mathbf{C}$ **do**
10. update the uncovered wall set $\mathbf{W}' = \mathbf{W} - \mathbf{S}_c$;
11. $\mathbf{\Gamma}$ = `AutoDeploySites` ($\mathbf{W}'$, $\mathbf{X} - \{c\}$, l_{un}, κ);
12. **if** $\mathbf{\Gamma}_{min}$ *is* $\varnothing$ *OR* $|\mathbf{\Gamma}_{min}| > |\mathbf{\Gamma}| + 1$ **then**
13. $\mathbf{\Gamma}_{\text{min}} \leftarrow \mathbf{\Gamma} \bigcap \{c\}$;
14. **return** $\mathbf{\Gamma}_{\text{min}}$;

C. A Dynamic Programming for Automated Cell Placement

According to the above, a dynamic programming for automated cell location selection is given in AutoDeploySites. From the CAPEX perspective, we don't have to design a network to cover the whole entire area. The algorithm stops when it meets the specified coverage percentage.

AutoDeploySites is a recursive algorithm. Lines 1–2 test if the coverage constraint is satisfied. Lines 3–4 select the walls whose serving cells to be determined. Lines 5–7 find the candidate cells and keep κ cells with maximum coverage areas. Line 8 initializes the solution set. Lines 9–13 are a relaxation process that tightens the upper bound of the solution's size in each step of recursive cycles. It's an output-sensitive framework whose running time and approximation ratio depend on the size of the output solution. If $\kappa = 1$, the proposed algorithm will be, in effect, a greedy algorithm.

If a wall can be covered by several cells in the solution, we choose the cell with the highest signal level as its only server. Let $\lambda_i (\lambda_i \leq 1)$ be the effective coverage rate of cell i defined as the ratio between the sizes of the actual covered set and the possible covered set $\mathbf{S}_i$.

Theorem 2: The worst-case running time of AutoDeploySites is $O(\frac{(\kappa^{|\mathcal{L}|}-1)(|\mathbf{X}||\mathbf{W}|+|\mathbf{W}|^2 \log |\mathbf{W}|)}{k-1})$. If $\kappa = 1$, the worst-case time is $O(|\mathcal{L}||\mathbf{X}||\mathbf{W}| + |\mathcal{L}||\mathbf{W}|^2 \log |\mathbf{W}|)$, and the upper limit of

TABLE I
5 G SIMULATION PARAMETERS FOR MMWAVE

Parameters	Values
Carrier frequency (GHz)	28, 39, 60
Tx power of reference signal (dBm)	20
Tx antenna gain (dBi)	20(Scenario1), 35(Scenario2)
Threshold of RSRP (dBm)	-95
Rain attenuation (dB/km)	3.45
Fading margin (dB)	5.1 (LOS), 10 (NLOS)
Other Losses (dB)	6
Permittivity	5.31
Height of TX antenna (m)	10
Height of RX antenna (m)	1.5
Channel model	see Section II-C

the ratio between the approximation and the optimal solutions is $\frac{\max\{|\mathbf{S}|:\mathbf{S}\in\mathcal{F}\}}{\min\{\lambda_i|\mathbf{S}_i|:\mathbf{S}_i\in\mathcal{L}\}}$.

Proof of Theorem 2. The proof is given in Appendix D.

IV. PERFORMANCE EVALUATION

A. Evaluation Scenario

We used C++ to develop our proposed cell planning framework and MATLAB to do data analysis, where 5 G simulation parameters are presented in Table I. We neglect the atmospheric attenuation and foliage losses in small cells. In this section, we consider two scenarios to be planned, as illustrated in Fig. 8 and Fig. 9, respectively.

1) *Scenario 1:* The hypothetical planning area is a $400 \times 400\text{m}^2$, on which there have been 64 building blocks distributed. Each building square is 40 m long, 20 m wide, 15 m high and randomly oriented.
2) *Scenario 2:* we relate the proposed algorithm to a real planning scenario by considering a central urban area of Beijing city. The red polygon region to be planned is about 3500×2000 m^2.

Generally speaking, the antennas of BS can't be installed anywhere, but often on roofs, walls, lampposts, bus stop boards of buildings, or that kind of places. In this work, we suppose antennas are mounted on the outer walls of buildings, as depicted in Fig. 8.

B. Results of the Hypothetical Scenario

We first tested the solution results for the hypothetical area which distributes very dense buildings. To avoid boundary effect, we have excluded the strips of 10 m wide along the border in the test scenario. Results are reported for the outdoor coverage in the central area of 380×380 m^2. The aim is to determine the locations of small cells for mmW in a highly dense buildings scenario.

Fig. 10 shows the reported SC locations and heatmaps where the signal levels are depicted based on a colour palette in the deployment budget of 8 small cells. Most of all cells are located on the corners of building block which can be explained by the fact that these cells have better chances to be chosen by the proposed algorithm due to their broader sights. From [9], [11], [14], mmW suffers from very high attenuation especially in the NLOS propagation environment. The wireless waves transmitted from the cells located on the corners of buildings can travel further in directional LOS link than others, which means they are expected to have a wider coverage area.

The diagrams of reference signal receiving power (RSRP) on 28 GHz, 39 GHz, 60 GHz frequencies are presented in Fig. 10(a)–(c), respectively. The whole "heat" goes down as the frequency gets higher, as seen in the heatmap. As discussed in Section II, the propagation loss becomes larger in the higher spectrum.

Fig. 11 shows the SC locations and heatmaps of SINR, similar to RSRP, they are also depicted based on a colour palette. Due to the weak interference of the adjacent SCs, the SINR in the area close to the SC is relatively high. On the contrary, in the area far away from the SC, the interference is strong and the SINR is relatively low. Although the SINR in the area far from SCs and the corner area blocked by obstacles is small due to the interference of adjacent SCs, the SINR in most places is still in 0–20 dB.

In order to analyze coverage quality, the whole complementary cumulative distribution functions of RSRP have been computed, as shown in Fig. 12. It should be noted that we collected the RSRP values of the outdoor grids with 1 m resolution. Without loss of generality, we set the threshold of RSRP in good quality as -95 dBm. We can observe that 8 SCs provide 94%, 92%, 87% of the planning area in good coverage quality on 28 GHz, 39 GHz and 60 GHz frequencies, respectively. The coverage indicator is better on 28 GHz than 60 GHz by approximately 5% within the same cost budget. We also output the results of the grid-based approach for comparison, which are drawn by dashed lines in Fig. 12. We can observe that the results of the grid-based method are slightly better than the proposed method, which provide 95%, 92.5%, 89% of the planning area in good coverage quality on three different frequencies. It is indicated that our method can also achieve the coverage quality almost equal to the grid-based method and is very practical. The CCDFs of SINR have also been computed in Fig. 13, we can observe that the SINR in 94%, 94.5% and 90% of the planning area could be greater than -5 dB on 28 GHz, 39 GHz and 60 GHz respectively. Though the SINR is better on 28 GHz and 39 GHz than 60 GHz, it is still acceptable on 60 GHz.

Similar tests were applied for hypothetical environment subject to a reserve coverage percentage of 92%. The coverage constraint here refers to the percentage of covered walls computed by vector-based algorithms in the solution. The results are depicted in Figs. 14–17, where we can deduct similar conclusions. And this test was conducted under the given coverage constraint, so we did not make comparison with the gird-based method on coverage rate. However, when the frequency of the SCs increases, the density of deployed SCs also increases to counteract the effects of higher loss under the same coverage constraint. We noticed, in Fig. 16, the actual area coverage percentage is about 97% which is greater than the preset threshold 92%. It is because the coverage constraint is approximately the border coverage rate that is expected to be smaller than the area coverage rate.

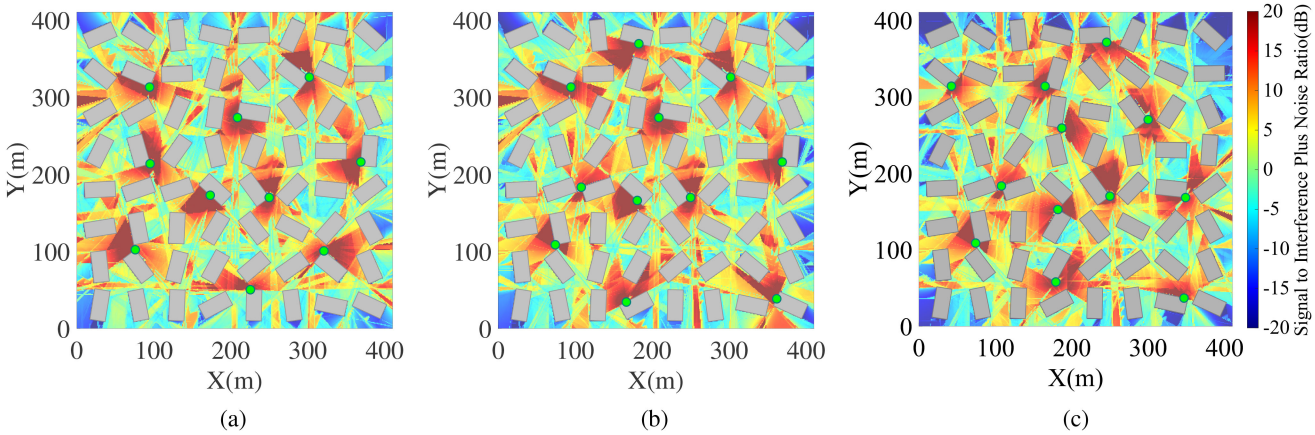

Fig. 11. Output cell locations and composite SINR of 8 SCs assuming $\kappa = 4$. (a) 28 GHz. (b) 39 GHz. (c) 60 GHz.

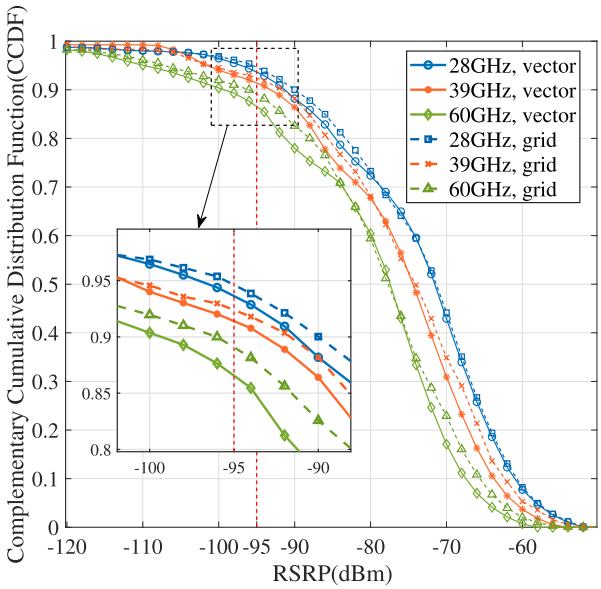

Fig. 12. Complementary cumulative distribution function of RSRP in the deployment of 8 SCs assuming $\kappa = 4$.

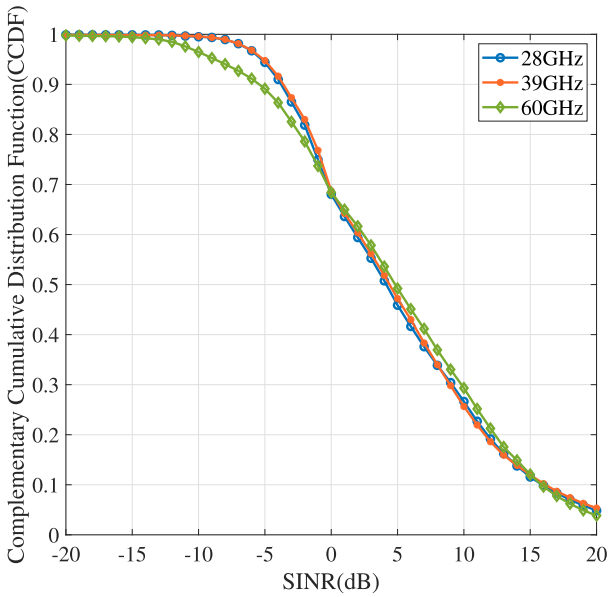

Fig. 13. Complementary cumulative distribution function of SINR in the deployment of 8 SCs assuming $\kappa = 4$.

C. Discussion on Algorithm Efficiency

The proposed framework is composed of computations with wall blocking, coverage evaluations and a tree traversal. So, the total running time depends on the number of walls, SCs in the solution, tree node's branches.

The relationship between the number of SCs in the solution and the number of a tree node's branches has been generated, as represented in Fig. 18, in order to test the convergence of the algorithm. Results show that it achieves convergence within κ less than 4 on the scale of a dozen SCs. The network size is associated with the area, the operating frequency, and the target value of network coverage quality as shown in Fig. 19. The algorithm outputs the SCs that number from a few with 0.75 of coverage rate to a dozen with 0.95 of coverage rate. Specifically, our algorithm will give the deployment of 10 small cells to meet the coverage rate of 83%–86% on 60 GHz. When the coverage constraint increases to 87%, our algorithm will output 11 small cells' deployment. The illustrated increasing curves are not smooth, since the coverage rate increases by several percentage points after adding one SC into a small planning area.

For the hypothetical scenario, the proposed algorithm based on vectors is compared to the one based on grids in running time. It ran in a physical machine with a CPU of 1.99 GHz and a memory of 16 GB. For the budget of 8 cells, the proposed algorithm executed 2 seconds, about 4 or 5 times faster compared to 9 seconds with 5 m resolution and 29 seconds with 1 m resolution from the one based on grid-map, as illustrated in Fig. 20. Much time reduction can be explained by the fact that the calculation amount of signal level evaluation by vectors is less than the one by grids. With the increase of resolution, the algorithm based on grid-map slows the efficiency down significantly.

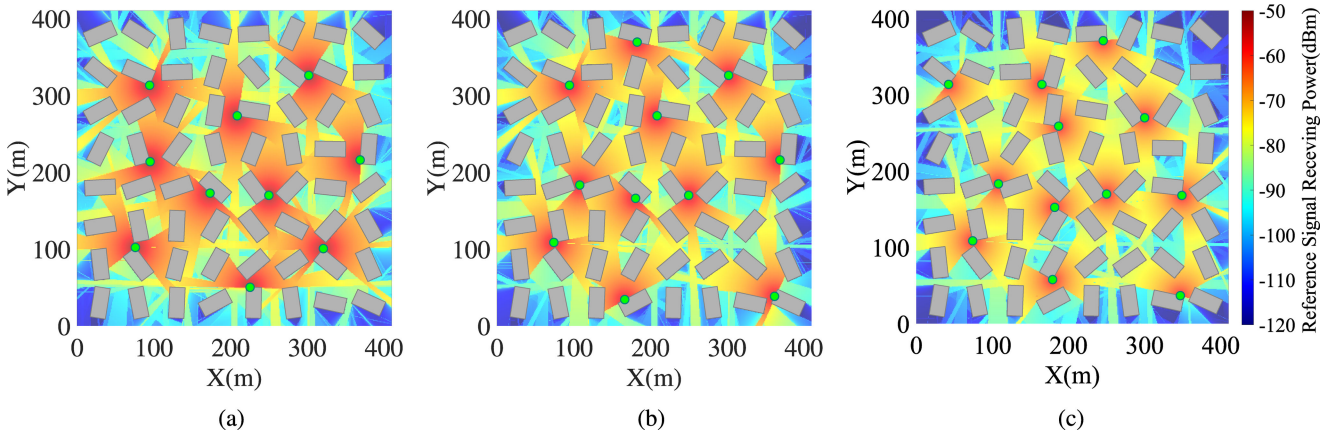

Fig. 14. Output cell locations and composite RSRP under the condition of 92% border coverage percentage assuming $\kappa = 4$. (a) 28 GHz. (b) 39 GHz. (c) 60 GHz.

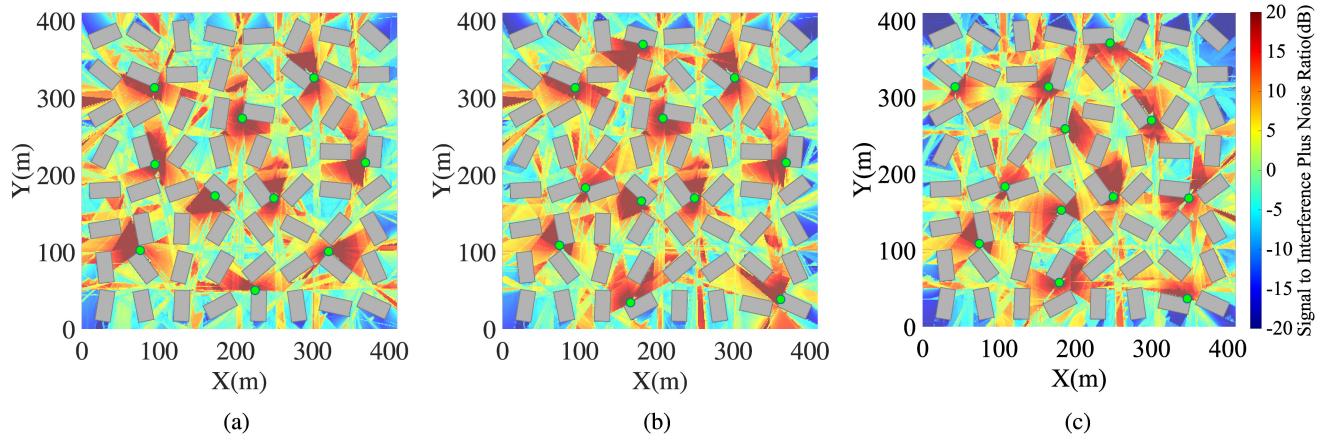

Fig. 15. Output cell locations and composite SINR under the condition of 92% border coverage percentage assuming $\kappa = 4$. (a) 28 GHz. (b) 39 GHz. (c) 60 GHz.

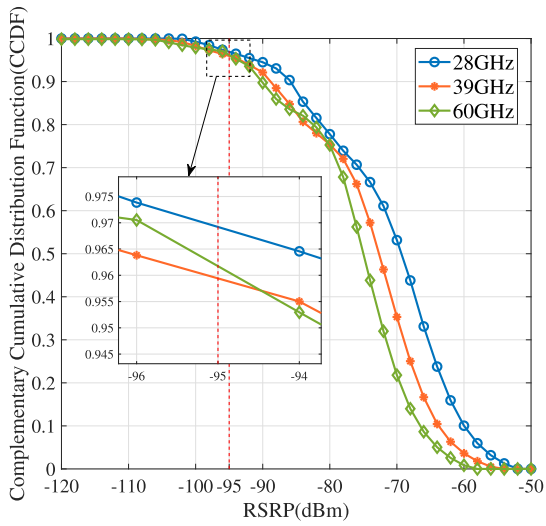

Fig. 16. Complementary cumulative distribution function of RSRP under the condition of 92% border coverage percentage assuming $\kappa = 4$.

D. Experiment of Real Planning Scenario

After some hypothetical scenarios, we related the proposed algorithm to a real planning scenario in Beijing city. We considered one of the central urban areas where there is a high concentration of buildings. RSRP indicators of the areas in LOS and NLOS within two reflections and diffractions are to be evaluated. The signal level indoor is also calculated using the outdoor-to-indoor penetration loss modelled as [39]:

$$PL_{\text{O2I}} = PL_{\text{outdoor}} + 5 + 0.5d_{\text{in}} - 10\log\left(0.7 \cdot 10^{\frac{-(23+0.3f)}{10}} + 0.3 \cdot 10^{\frac{-(5+4f)}{10}}\right), \tag{11}$$

where PL_{outdoor} is given in Section II-C, f is the frequency in GHz, and d_{in} is the indoor propagation distance. The algorithm outputs 45 cells under the constraint of 90% outdoor coverage on 28 GHz. We generated the images rendered with the RSRP and SINR of each pixel covered by all planned cells, as shown in Fig. 21 and Fig. 22. We noticed that cells non-uniformly distribute on the area due to the different densities of buildings in different parts. As shown, there are denser deployed cells in area B than area A. The achieved solution might not be the best one because we reserved quite limited branches ($\kappa = 2$) of a tree node. It might take a great amount

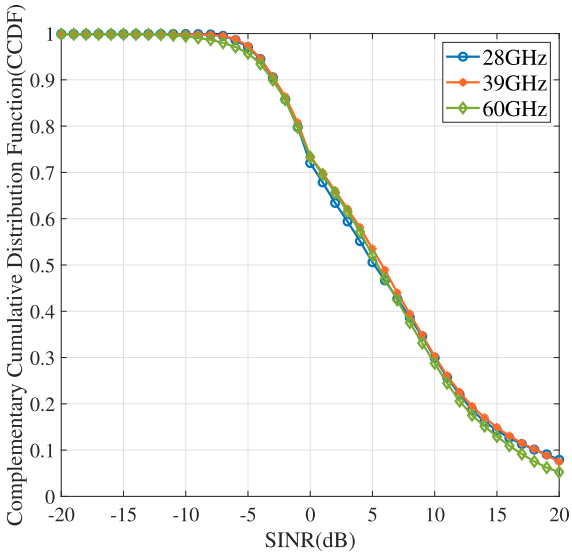

Fig. 17. Complementary cumulative distribution function of SINR under the condition of 92% border coverage percentage assuming $\kappa = 4$.

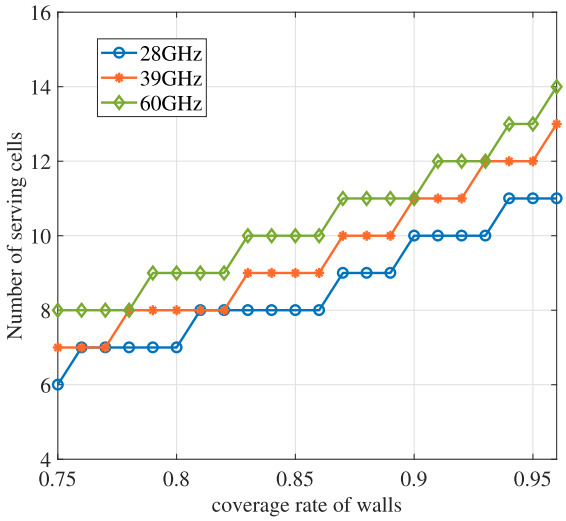

Fig. 19. Number of small cells in the solution with the increasing target value of coverage rate assuming $\kappa = 4$.

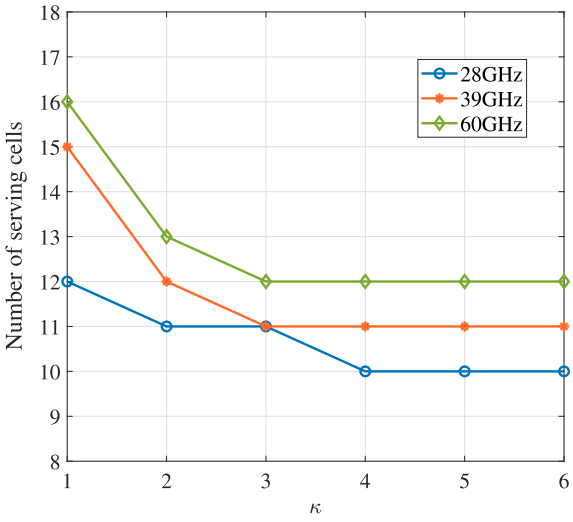

Fig. 18. Number of small cells in the solution with κ tree node's branches assuming 92% coverage percentage.

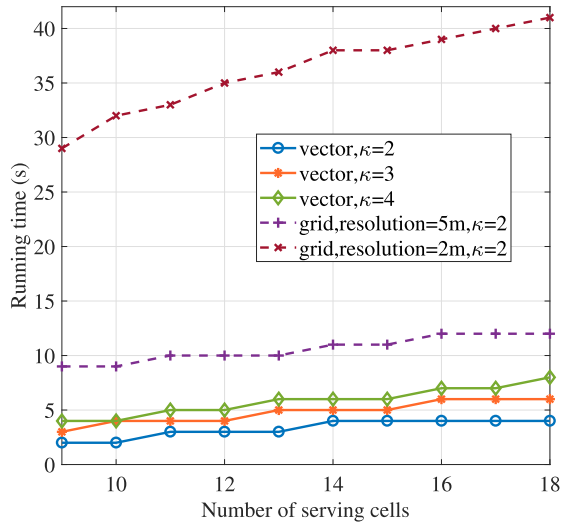

Fig. 20. Comparison between the proposed vector-based algorithm and the grid-based one in terms of running time (the operating frequency is 60 GHz).

of time for a large value of κ when planning a large-scaled network.

In Fig. 21 and Fig. 22, we observed that most outdoor areas get a good coverage quality, while it's poor indoors. There exists a strong limitation of outdoor-to-indoor penetration for mmW. In this sense, planning a network with indoor coverage by outdoor mmW cells is ineffective. In Fig. 23, we generated coverage statistics on different types of areas. The outdoor part occupies about 68% of the planned area, while the indoor proportion is 32%. It can be noticed that less than 10% of the indoor area achieves good coverage quality where the RSRP is above -95 dBm, while nearly the whole outdoor area in LOS has a good quality and just a few outdoor parts in NLOS are covered with poor quality.

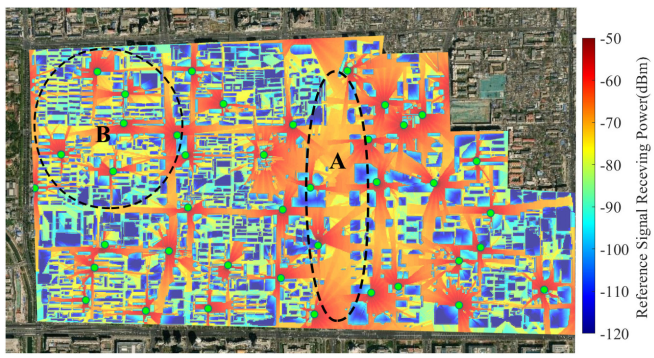

Fig. 21. Composite RSRP of all planned SCs.

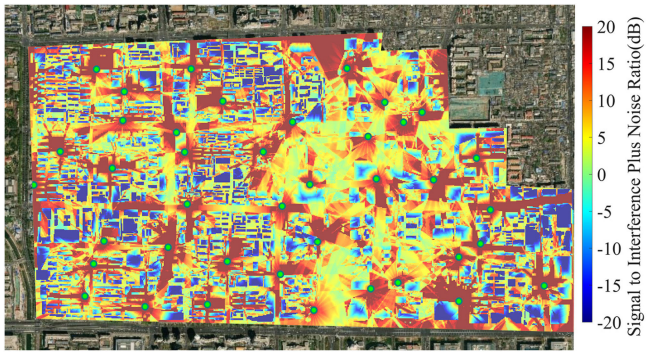

Fig. 22. Composite SINR of all planned SCs.

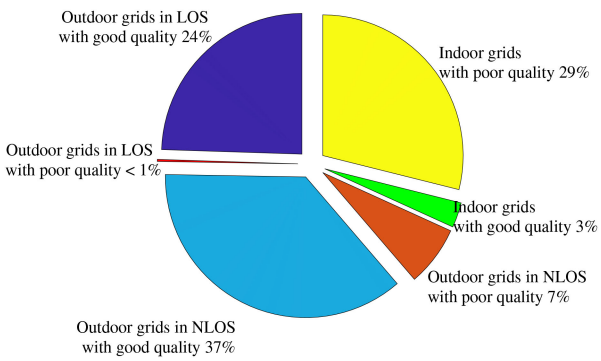

Fig. 23. Comparison on the coverage qualities of different kinds of areas.

V. Conclusion

Operators may incur high terrain costs if small mmW cells are widely deployed to improve network quality in a dense urban area due to the poor propagation performance. We proposed a novel algorithm to automatically deploy the number and location of small cells with mmW in dense urban subjects to the coverage constraint. The problem was solved by a vector-based model of network coverage and an optimal search method based on dynamic programming.

Simulation results show that the proposed algorithm can optimize the number and location of small-cell BSs, under the condition of cost budget or coverage percentage, in the scenario of dense buildings. The process was 4 or 5 times faster than the one based on grid-map. In order to reduce computation time, the size of the search tree should be reduced to a comparatively small value to obtain approximate solutions, however, for a large-scaled network.

In the future, we propose to improve the search technique based on the vector model. Clustering or divide-and-conquer approaches are suggested to be applied for large-scaled scenarios. For the deployment of SCs, energy efficiency is also an important metric that needs to be considered. It is worth studying whether the proposed vector-based model can be used for the deployment of SC with energy efficiency as the optimization target. Moreover, intelligent reflecting surfaces (IRS) can reflect the income signal after modulation intelligently which is a good solution in dense urban environments. How to use the proposed algorithm to solve the deployment problem of IRS is worthy of further investigation.

Appendix A
Proof of Theorem 1

Proof: Assume one wall is covered only by one cell. If multiple received powers of signals from more than one cell are higher than the required threshold, the one with the highest level is the only best server. Let $\mathbf{S}_i$ be the wall set covered by cell i, then $\mathbf{S}_i \bigcap \mathbf{S}_j = \varnothing, \forall i \neq j$.

Given an optimal solution $\mathbf{\Gamma}_{1,K} = \{n_1, \cdots, n_K\}$ where n_i denotes the cell number and $\mathbf{\Gamma}_{1,K} \subset \mathbf{X}$, without loss of generality, we decompose the optimal solution $\mathbf{\Gamma}_{1,K}$ into two set $\mathbf{\Gamma}_{1,L}$ and $\mathbf{\Gamma}_{L+1,K}$ where $1 \leq L \leq K$. Then $\mathbf{\Gamma}_{1,L}$ and $\mathbf{\Gamma}_{L+1,K}$ are respectively the optimal solutions to cover the walls $\bigcup_{i\in\mathbf{\Gamma}_{1,L}} \mathbf{S}_i$ and $\bigcup_{i\in\mathbf{\Gamma}_{L+1,K}} \mathbf{S}_i$.

The above conclusion can be proved by reduction to absurdity as follows.

Suppose $\mathbf{\Gamma}'$ is the optimal solution to cover the walls $\bigcup_{i\in\mathbf{\Gamma}_{1,L}} \mathbf{S}_i$, and $|\mathbf{\Gamma}'| < |\mathbf{\Gamma}_{1,L}| = L$, then $\mathbf{\Gamma}' \bigcup \mathbf{\Gamma}_{L+1,K}$ is the optimal solution of the whole problem.

$\because |\mathbf{\Gamma}' \bigcup \mathbf{\Gamma}_{L+1,K}| \leq |\mathbf{\Gamma}'| + |\mathbf{\Gamma}_{L+1,K}| < |\mathbf{\Gamma}_{1,L}| + |\mathbf{\Gamma}_{L+1,K}| = K$, contradicting $\mathbf{\Gamma}_{1,K}$ is an optimal solution,

$\therefore \mathbf{\Gamma}_{1,L}$ is an optimal solution to cover the walls $\bigcup_{i\in\mathbf{\Gamma}_{1,L}} \mathbf{S}_i$.

Symmetrically, $\mathbf{\Gamma}_{L+1,K}$ is an optimal solution to cover the walls $\bigcup_{i\in\mathbf{\Gamma}_{L+1,K}} \mathbf{S}_i$.

Thus, this problem has an optimal substructure. □

Appendix B
Proof of Lemma 1

Proof: Take a look first at the running time of the subprocedure UpdateStatus. Lines 14 and 22 take $O(\log n)$ time using operations of a binary tree. The other lines just take constant time.

The running time of FindWalls is worked out as follows.

Lines 2–4 take constant time for initial operations.

Lines 5–7 take $O(n \log n)$ time using heapsort.

Lines 8–10 execute $2n$ loops. It takes $O(n \log n)$ time as Update_Status is called once per iteration.

Thus, the total time of FIND_WALLS is $O(n \log n)$. □

Appendix C
Proof of Lemma 2

Proof:

Line 2 takes $O(1)$ time for initial operation.

Line 3 takes $O(1)$ time for link budget.

Line 4 takes $O(|\mathbf{W}| \log |\mathbf{W}|)$ according to Lemma 1 since it calls FindWalls.

The loop of lines 5-11 iterates $|\mathbf{W}_{\text{LOS}}|$ times, not exceeding $|\mathbf{W}|$. It takes totally $O(|\mathbf{W}|^2 \log |\mathbf{W}|)$ time since each iteration calls FindWalls 3 times.

The last line takes at most $O(|\mathbf{X}| \cdot |\mathbf{W}|)$ time.

So, The worst-case time is $O(|\mathbf{X}| \cdot |\mathbf{W}| + |\mathbf{W}|^2 \log |\mathbf{W}|)$ in all. □

APPENDIX D
PROOF OF THEOREM 2

Proof: Proof of running time:

Lines 3-4 take $O(|\mathbf{W}|\log|\mathbf{W}|)$ time by the algorithm of computing a convex hull in [42].

Line 5 takes $O(|\mathbf{X}|\cdot|\mathbf{W}|+|\mathbf{W}|^2\log|\mathbf{W}|)$ time in the worst case according to Lemma 2.

Line 6 takes $O(|\mathbf{X}|\cdot|\mathbf{W}|)$ time in the worst case.

Lines 8–12 execute loops to expand the search tree. The number of loops depends on κ, and the depth of the tree depends on $|\boldsymbol{\mathcal{L}}|$ or $|\boldsymbol{\Gamma}|$. The total number of nodes is $\sum_{i=0}^{|\boldsymbol{\mathcal{L}}|-1}\kappa^i=\frac{\kappa^{|\boldsymbol{\mathcal{L}}|}-1}{\kappa-1}$. Thus, the worst-case running time in all is $O(\frac{(\kappa^{|\boldsymbol{\mathcal{L}}|}-1)(|\mathbf{X}||\mathbf{W}|+|\mathbf{W}|^2\log|\mathbf{W}|)}{k-1})$. If $\kappa=1$, the algorithm is simplified as the greedy case in which the search tree has $|\boldsymbol{\mathcal{L}}|$ nodes and the worst-case time is $O(|\boldsymbol{\mathcal{L}}||\mathbf{X}||\mathbf{W}|+|\boldsymbol{\mathcal{L}}||\mathbf{W}|^2\log|\mathbf{W}|)$.

Proof of the approximation ratio:

Let $\boldsymbol{\Gamma}^*$ be the optimal solution and $\boldsymbol{\mathcal{L}}^*$ be the family of the optimal coverage sets. Like the set-covering problem in [22], we assign a cost of 1 to each cell and distribute the cost over the walls covered by the cell. For each $w\in\mathbf{W}$, let c_w represent the cost assigned to the wall w. If w is covered by cell i, then $c_w=\frac{1}{\lambda_i|\mathbf{S}_i|}$.

Each step of Automatically_Deploy_Sites selects one serving cell and assigns a cost of 1, so

$$|\boldsymbol{\Gamma}|=\sum_{w\in\mathbf{W}}c_w. \tag{12}$$

Because $\boldsymbol{\mathcal{L}}^*$ includes all walls, each $w\in\mathbf{W}$ is in at least one set of $\boldsymbol{\mathcal{L}}^*$. So,

$$\sum_{w\in\mathbf{W}}c_w\le\sum_{\mathbf{S}\in\mathcal{L}^*}\sum_{w\in\mathbf{S}}c_w, \tag{13}$$

$$\begin{aligned}\therefore\sum_{w\in\mathbf{S}}c_w&\le|\mathbf{S}|\cdot\max\{c_w:w\in\mathbf{S}\}\\&\le|\mathbf{S}|\cdot\frac{1}{\min\{\lambda_i|\mathbf{S}_i|:|\mathbf{S}|\in\mathcal{L}\}}\\&\le\frac{\max\{|\mathbf{S}|:|\mathbf{S}|\in\mathcal{L}^*\}}{\min\{\lambda_i|\mathbf{S}_i|:|\mathbf{S}|\in\mathcal{L}\}}\\&\le\frac{\max\{|\mathbf{S}|:|\mathbf{S}|\in\mathcal{F}\}}{\min\{\lambda_i|\mathbf{S}_i|:|\mathbf{S}|\in\mathcal{L}\}}.\end{aligned} \tag{14}$$

From equations (12), (13) and (14), it follows that

$$\begin{aligned}|\boldsymbol{\Gamma}|=\sum_{w\in\mathbf{W}}c_w&\le\sum_{\mathbf{S}\in\mathcal{L}^*}\frac{\max\{|\mathbf{S}|:\mathbf{S}\in\mathcal{F}\}}{\min\{\lambda_i|\mathbf{S}_i|:\mathbf{S}_i\in\mathcal{L}\}}\\&\le|\mathcal{L}^*|\cdot\frac{\max\{|\mathbf{S}|:\mathbf{S}\in\mathcal{F}\}}{\min\{\lambda_i|\mathbf{S}_i|:\mathbf{S}_i\in\mathcal{L}\}}\\&=|\boldsymbol{\Gamma}^*|\cdot\frac{\max\{|\mathbf{S}|:\mathbf{S}\in\mathcal{F}\}}{\min\{\lambda_i|\mathbf{S}_i|:\mathbf{S}_i\in\mathcal{L}\}},\end{aligned}$$

$$\therefore\frac{|\boldsymbol{\Gamma}|}{|\boldsymbol{\Gamma}^*|}\le\frac{\max\{|\mathbf{S}|:\mathbf{S}\in\mathcal{F}\}}{\min\{\lambda_i|\mathbf{S}_i|:\mathbf{S}_i\in\mathcal{L}\}}.$$

□

REFERENCES

[1] Q. Q. Wu, G. Y. Li, W. Chen, D. W. K. Ng, and R. Schober, "An overview of sustainable green 5G networks," *IEEE Wireless Commun.*, vol. 24, no. 4, pp. 72–80, Aug. 2017.

[2] "Cisco Annual Internet Report (2018–2023)," in Cisco Annual Internet Report (2018–2023) White Paper, pp. 1–35, Mar. 9, 2020.

[3] A. Al-Dulaimi, S. Al-Rubaye, J. Cosmas, and A. Anpalagan, "Planning of ultra-dense wireless networks," *IEEE Netw.*, vol. 31, no. 2, pp. 90–96, Mar./Apr. 2017.

[4] A. Taufique, M. Jaber, A. Imran, Z. Dawy, and E. Yacoub, "Planning wireless cellular networks of future: Outlook, challenges and opportunities," *IEEE Access*, vol. 5, pp. 4808–4832, 2017.

[5] F. Farias *et al.*, "Cost-and energy-efficient backhaul options for heterogeneous mobile network deployments," *Photonic Netw. Commun.*, vol. 32, no. 3, pp. 422–437, Dec. 2016.

[6] S. Rahmatia, D. Martin, M. Ismail, O. Nur Samijayani, D. Astharini, and R. Safitri, "Automatic cell planning of LTE FDD 1800 MHz network in Klaten, Central Java," in *Proc. 2nd Int. Conf. Elect., Commun. Comput. Eng.*, 2020, pp. 1–6.

[7] R. Chen, X. Zhang, J. Wang, Q. Cui, W. Xu, and M. Pan, "Data-driven small cell planning for traffic offloading with users' differential privacy," in *Proc. IEEE Int. Conf. Commun.*, 2020, pp. 1–6.

[8] Y. Ozcan, J. Oueis, C. Rosenberg, R. Stanica, and F. Valois, "Robust planning and operation of multi-cell homogeneous and heterogeneous networks," *IEEE Trans. Netw. Service Manag.*, vol. 17, no. 3, pp. 1805–1821, Sep. 2020.

[9] T. S. Rappaport, Y. C. Xing, G. R. MacCartney, A. F. Molisch, E. Mellios, and J. H. Zhang, "Overview of millimeter wave communications for fifth-generation (5G) wireless networks-with a focus on propagation models," *IEEE Trans. Antennas Propag.*, vol. 65, no. 12, pp. 6213–6230, Dec. 2017.

[10] A. N. Uwaechia, N. M. Mahyuddin, M. F. Ain, N. M. A. Latiff, and N. F. Za'bah, "On the spectra efficiency of low-complexity and resolution hybrid precoding and combining transceivers for mmWave MIMO systems," *IEEE Access*, vol. 7, pp. 109259–109277, 2019.

[11] A. N. Uwaechia and N. M. Mahyuddin, "A comprehensive survey on millimeter wave communications for fifth-generation wireless networks: Feasibility and challenges," *IEEE Access*, vol. 8, pp. 62367–62414, 2020.

[12] S. Sun, T. S. Rappaport, M. Shafi, P. Tang, J. H. Zhang, and P. J. Smith, "Propagation models and performance evaluation for 5G millimeter-wave bands," *IEEE Trans. Veh. Technol.*, vol. 67, no. 9, pp. 8422–8439, Sep. 2018.

[13] J. Lee, K. W. Kim, M. D. Kim, J. J. Park, Y. K. Yoon, and Y. J. Chong, "Millimeter-wave directional-antenna beamwidth effects on the ITU-R building entry loss (BEL) propagation model," *ETRI J.*, vol. 42, no. 1, pp. 7–16, Feb. 2020.

[14] K. W. Kim, M. D. Kim, J. Y. Lee, J. J. Park, Y. K. Yoon, and Y. J. Chong, "Millimeter-wave diffraction-loss model based on over-rooftop propagation measurements," *ETRI J.*, vol. 42, no. 6, pp. 827–836, Dec. 2020.

[15] *Attenuation by Atmospheric Gases*, Recommendation ITU-R P.676-10, Sep. 2013.

[16] X. H. Ge, S. Tu, G. Q. Mao, C. X. Wang, and T. Han, "5G ultra-dense cellular networks," *IEEE Wireless Commun.*, vol. 23, no. 1, pp. 72–79, Feb. 2016.

[17] Y. J. Chen, M. Ding, and D. Lopez-Perez, "Performance of ultra-dense networks with a generalized multipath fading," *IEEE Wireless Commun. Lett.*, vol. 8, no. 5, pp. 1419–1422, Oct. 2019.

[18] L. Chiaraviglio *et al.*, "Planning 5G networks under EMF constraints: State of the art and vision," *IEEE Access*, vol. 6, pp. 51021–51037, 2018.

[19] M. Kamel, W. A. Hamouda, and A. Youssef, "Uplink coverage and capacity analysis of mMTC in ultra-dense networks," *IEEE Trans. Veh. Technol.*, vol. 69, no. 1, pp. 746–759, Jan. 2020.

[20] L. C. Goncalves, P. Sebastiao, N. Souto, and A. Correia, "5G mobile challenges: A feasibility study on achieving carbon neutrality," in *Proc. 23rd Int. Conf. Telecommun.*, 2016, pp. 1–5.

[21] T. S. Rappaport *et al.*, "Millimeter wave mobile communications for 5G cellular: It will work!," *IEEE Access* vol. 1, pp. 335–349, 2013.

[22] T. H. Cormen, C. E. Leiserson, R. L. Rivest, and C. Stein, *Introduction to Algorithms*. Cambridge, MA, USA: MIT Press, 2009.

[23] S. Hurley, "Planning effective cellular mobile radio networks," *IEEE Trans. Veh. Technol.*, vol. 51, no. 2, pp. 243–253, Mar. 2002.

[24] L. Zhang and Z. H. Peng, "An improved genetic algorithm analysis and application study for urban microcellular network planning," *J. Intell. Fuzzy Syst.*, vol. 35, no. 3, pp. 2805–2811, 2018.

[25] H. Ganame, Y. Z. Liu, H. Ghazzai, and D. Kamissoko, "5G base station deployment perspectives in millimeter wave frequencies using meta-heuristic algorithms," *Electronics*, vol. 8, no. 11, Nov. 2019, Art. no. 1318.
[26] H. Ghazzai, E. Yaacoub, M. S. Alouini, Z. Dawy, and A. Abu-Dayya, "Optimized LTE cell planning with varying spatial and temporal user densities," *IEEE Trans. Veh. Technol.*, vol. 65, no. 3, pp. 1575–1589, Mar. 2016.
[27] Y. C. Wang and S. Lee, "Small-cell planning in LTE HetNet to improve energy efficiency," *Int. J. Commun. Syst.*, vol. 31, no. 5, Mar. 2018, Art. no. e3492.
[28] M. Naderi Soorki, W. Saad, and M. Bennis, "Optimized deployment of millimeter wave networks for in-venue regions with stochastic users' orientation," *IEEE Trans. Wireless Commun.*, vol. 18, no. 11, pp. 5037–5049, Nov. 2019.
[29] A. Godinho *et al.*, "A novel way to automatically plan cellular networks supported by linear programming and cloud computing," *Appl. Sci.-Basel*, vol. 10, no. 9, May 2020, Art. no. 3072.
[30] U. Challita, Z. Dawy, G. Turkiyyah, and J. Naoum-Sawaya, "A chance constrained approach for LTE cellular network planning under uncertainty," *Comput. Commun.*, vol. 73, pp. 34–45, 2016.
[31] W. T. Zhao, S. W. Wang, C. G. Wang, and X. B. Wu, "Approximation algorithms for cell planning in heterogeneous networks," *IEEE Trans. Veh. Technol.*, vol. 66, no. 2, pp. 1561–1572, Feb. 2017.
[32] L. Ma, X. Wang, M. Huang, Z. Lin, L. Tian, and H. Chen, "Two-level master-slave RFID networks planning via hybrid multiobjective artificial bee colony optimizer," *IEEE Trans. Syst., Man, Cybern. Syst.*, vol. 49, no. 5, pp. 861–880, May 2019.
[33] P. Munoz, O. Sallent, and J. Perez-Romero, "Self-dimensioning and planning of small cell capacity in multitenant 5G networks," *IEEE Trans. Veh. Technol.*, vol. 67, no. 5, pp. 4552–4564, May 2018.
[34] L. Al-Kanj, W. El-Beaino, A. M. El-Hajj, and Z. Dawy, "Optimized joint cell planning and BS on/off switching for LTE networks," *Wireless Commun. Mobile Comput.*, vol. 16, no. 12, pp. 1537–1555, 2016.
[35] M. Dong, T. Kim, J. Wu, and E. W. M. Wong, "Cost-efficient millimeter wave base station deployment in manhattan-type geometry," *IEEE Access*, vol. 7, pp. 149959–149970, 2019.
[36] V. B. Nikam, A. Arora, D. Lambture, J. Zaveri, P. Shinde, and M. More, "Optimal positioning of small cells for coverage and cost efficient 5G network deployment: A smart simulated annealing approach," in *Proc. IEEE 3rd 5G World Forum*, 2020, pp. 454–459.
[37] H. Leem, J. Kim, B. H. Jung, and D. K. Sung, "Spectral-, energy-, & cost-efficient deployment of small cells in a HetNet topology," in *Proc. IEEE Int. Conf. Commun.*, 2014, pp. 4042–4047.
[38] *Effects of Building Materials and Structures on Radiowave Propagation Above About 100 MHz*, Recommendation ITU-R P.2040-1, Jul. 2015.
[39] "Study on channel model for frequencies from 0.5 to 100 GHz," *3GPP, Sophia Antipolis Cedex, France*, Tech. Rep. 38.901, vol. V16.0.0, Oct. 2019.
[40] J. B. Keller, "Geometrical theory of diffraction," *J. Opt. Soc.*, vol. 52, no. 2, pp. 116–130, 1962.
[41] M. A. Ouamri, M. Azni, and M. Oteşteanu, "Coverage analysis in two-tier 5G hetnet based on stochastic geometry with interference coordination strategy," *Wireless Pers. Commun.*, vol. 121, no. 4, pp. 3213–3222, 2021.
[42] M. D. Berg, O. Cheong, M. V. Kreveld, and M. Overmars, *Computational Geometry: Algorithms and Applications*, 3rd ed. Berlin, Germany: Springer, 2008.

Jianming Zhang received the B.E. degree in communication engineering and the Ph.D. degree in communication system from the Beijing University of Posts and Telecommunications, Beijing, China, in 1999 and 2004, respectively. In 2004, he joined the School of Electronic Engineering, Beijing University of Posts and Telecommunications, where he is currently an Associate Professor with Communication and Network Center. His current research interests wireless network planning, wireless channel modeling, machine learning, and Big Data applications.

Deru Zhang received the B.S. degree in mathematics and applied mathematics from Northwestern Polytechnical University, Xi'an, China, in 2020. He is currently working toward the master's degree with the School of Electronic Engineering, Beijing University of Posts and Telecommunications, Beijing, China. His current research interests include wireless network optimization, wireless channel modeling, and intelligent reflecting surface.

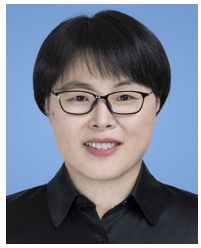

Juanjuan Sun received the B.E. degree in electronics and information systems from Jilin University, Changchun, China, and the M.E. degree and the Ph.D. degree in information and communication system from the Beijing University of Posts and Telecommunications, Beijing, China, in 2002 and 2007, respectively. In 2007, she joined the School of Electronic Engineering, Beijing University of Posts and Telecommunications, where she is currently an Associated Professor with Communication and Network Center. Her current research interests include theories and applications of wireless communication networks.